Cholinergic left-right asymmetry in the habenulo-interpeduncular pathway

Elim Hong[a], Kirankumar Santhakumar[a,1], Courtney A. Akitake[a], Sang Jung Ahn[a,2], Christine Thisse[b], Bernard Thisse[b], Claire Wyart[c], Jean-Marie Mangin[d,3], and Marnie E. Halpern[a,3]

[a]Department of Embryology, Carnegie Institution for Science, Baltimore, MD 21218; [b]Department of Cell Biology, Health Sciences Center, University of Virginia, Charlottesville, VA; [c]Institut du Cerveau et de la Moelle Épinière, Hôpital de la Pitié-Salpêtrière, F-75013, Institut National de la Santé et de la Recherche Médicale Unité Mixte de Recherche S975, Centre National de la Recherche Scientifique Unité Mixte de Recherche 7225, Université Pierre et Marie Curie, 75005 Paris, France; and [d]Institut National de la Santé et de la Recherche Médicale U952, Université Pierre et Marie Curie, 75005 Paris, France

Edited by Igor B. Dawid, The Eunice Kennedy Shriver National Institute of Child Health and Human Development, National Institutes of Health, Bethesda, MD, and approved November 12, 2013 (received for review October 18, 2013)

The habenulo-interpeduncular pathway, a highly conserved cholinergic system, has emerged as a valuable model to study left-right asymmetry in the brain. In larval zebrafish, the bilaterally paired dorsal habenular nuclei (dHb) exhibit prominent left-right differences in their organization, gene expression, and connectivity, but their cholinergic nature was unclear. Through the discovery of a duplicated cholinergic gene locus, we now show that *choline acetyltransferase* and *vesicular acetylcholine transporter* homologs are preferentially expressed in the right dHb of larval zebrafish. Genes encoding the nicotinic acetylcholine receptor subunits α2 and β4 are transcribed in the target interpeduncular nucleus (IPN), suggesting that the asymmetrical cholinergic pathway is functional. To confirm this, we activated channelrhodopsin-2 specifically in the larval dHb and performed whole-cell patch-clamp recording of IPN neurons. The response to optogenetic or electrical stimulation of the right dHb consisted of an initial fast glutamatergic excitatory postsynaptic current followed by a slow-rising cholinergic current. In adult zebrafish, the dHb are divided into discrete cholinergic and peptidergic subnuclei that differ in size between the left and right sides of the brain. After exposing adults to nicotine, *fos* expression was activated in subregions of the IPN enriched for specific nicotinic acetylcholine receptor subunits. Our studies of the newly identified cholinergic gene locus resolve the neurotransmitter identity of the zebrafish habenular nuclei and reveal functional asymmetry in a major cholinergic neuromodulatory pathway of the vertebrate brain.

optogeneticis | tachykinin 1 | electrophysiology | addiction

Lateralization of brain function is found throughout the animal kingdom, yet knowledge of the underlying neural bases for left-right (L-R) specializations is limited. Multiple developmental mechanisms could account for differential neural activity, including asymmetry in cell number or density, in specification of neuronal types, or in connectivity. Increasing evidence suggests that L-R differences in neurotransmitter distribution also play an important role in lateralized behaviors.

The bilaterally paired habenular nuclei (Hb) of zebrafish provide a valuable model to study brain asymmetry. In larvae, the dorsal habenulae (dHb) [equivalent to medial habenular nuclei (mHb) of mammals] exhibit pronounced L-R differences in size, molecular properties, and connections with their midbrain target, the interpeduncular nucleus (IPN) (1–3). The Hb-IPN pathway connects limbic areas of the forebrain and midbrain (4), and has been implicated in nicotine addiction in mammals (5).

The mHb-IPN tract is a major cholinergic system across vertebrates (6–11); however, it is still unresolved whether this pathway is cholinergic in zebrafish. Cholinergic neurons are defined by the presence of choline acetyltransferase (ChAT), which synthesizes ACh from choline and acetyl CoA, and *vesicular acetylcholine transporter* (VAChT), which packages ACh into synaptic vesicles. The *chat* and *vacht* genes are situated in close proximity in a region defined as the "cholinergic gene locus" (CGL). Only one CGL has been annotated in the zebrafish genome. Transcripts for *chat* (12) and ChAT immunolabeling (13) are found in discrete nuclei throughout the larval brain but not in the habenular region. Moreover, labeling with antibodies directed against human ChAT led to conflicting results concerning the presence of immunoreactivity in the adult dHb (14, 15). Numerous genes encoding nicotinic acetylcholine receptor (nAChR) subunits are also expressed in the zebrafish larval brain (16, 17), but none have been detected in the IPN. This is surprising because the Hb-IPN tract exhibits the greatest number and type of nAChR subunits in the rodent brain (18–22). These discrepancies make it difficult to relate studies in zebrafish to mammalian habenular function.

We discovered a second CGL in zebrafish, which is predominantly transcribed in the right dHb of larvae. The asymmetrical Hb-IPN cholinergic pathway is functional because selective activation of channelrhodopsin-2 (ChR2) in the dHb produces slow cholinergic currents in IPN neurons. When adult fish are exposed to nicotine, neural activity, as assayed by *fos* expression, is chiefly found in the intermediate IPN (iIPN),

Significance

The forebrain habenular nuclei (Hb) and their connections to the midbrain interpeduncular nucleus (IPN) have emerged as a valuable model to study left-right differences in the zebrafish brain. However, whether this pathway is enriched in the neurotransmitter acetylcholine and involved in nicotine addiction as in mammals is unresolved. We discovered a duplicated cholinergic gene locus that is predominantly expressed in the right Hb at larval stages. Through electrophysiology and pharmacology, we show that this asymmetrical cholinergic pathway is functional. Moreover, specific nicotinic acetylcholine receptor subunits localize to the same subregions of the IPN that are activated by exposure of adults to nicotine. Our study firmly establishes the zebrafish as a valid model to study how Hb-IPN circuitry influences nicotine addiction.

Author contributions: E.H., K.S., J.-M.M., and M.E.H. designed research; E.H., K.S., S.J.A., and J.-M.M. performed research; C.W. assisted with optogenetics; E.H., K.S., C.A.A., S.J.A., C.T., B.T., and C.W. contributed new reagents/analytic tools; E.H., K.S., J.-M.M., and M.E.H. analyzed data; and E.H., J.-M.M., and M.E.H. wrote the paper.

The authors declare no conflict of interest.

This article is a PNAS Direct Submission.

Data deposition: The sequences reported in this paper have been deposited in the GenBank database (KF840480).

[1]Present address: Department of Genetic Engineering, Sri Ramaswamy Memorial University, Kattankulathur 603203, India.

[2]Present address: Aquatic Life Disease Control Division, National Fisheries Research and Development Institute (NFRDI), Busan 619-705, South Korea.

[3]To whom correspondence may be addressed. E-mail: jean-marie.mangin@inserm.fr or halpern@ciwemb.edu.

This article contains supporting information online at www.pnas.org/lookup/suppl/doi:10.1073/pnas.1319566110/-/DCSupplemental.

NEUROSCIENCE

a subregion innervated by cholinergic dHb neurons and enriched for *chrna2b* and *chrnb4* transcripts. Our findings provide compelling evidence for conservation of the cholinergic Hb-IPN pathway and reveal an unexpected L-R difference in neurotransmitter phenotype in the developing brain. Furthermore, this work establishes the zebrafish as a valid model for probing the molecular mechanisms and neuronal circuitry underlying nicotine addiction.

Results

Duplication of the CGL in Zebrafish. The CGL, containing *chat* and *vacht* genes, is found throughout the animal kingdom (Fig. S1*A*). A single locus, CGLa, was annotated in the zebrafish genome that maps to chromosome 13. The zebrafish *chata and vachta* [*solute carrier family 18, member 3a* (*slc18a3a*)] genes are expressed in overlapping patterns in the eye, hindbrain, and spinal cord, but not in the epithalamus (Fig. 1*A* and Fig. S2 *A–A″*).

In a screen to characterize tissue-specific expression of zebrafish cDNA clones (23), we discovered a second *vacht* gene, *vachtb* (*slc18a3b*) that maps to chromosome 12 and is closely related to *vachta* (74% amino acid similarity). In addition to being expressed in a bilaterally symmetrical pattern of neurons distributed throughout the brain and spinal cord, *vachtb* transcripts are concentrated in a discrete domain on the right side of the dorsal diencephalon (Figs. 1*B* and 2*B* and Fig. S2 *E–E″*).

Owing to the conserved nature of the CGL, the presence of a duplicated locus in other teleosts, and the syntenic relationship with flanking genes (Fig. S1*A*), we expected to find a second *chat* gene in close proximity to *vachtb*. However, a *chat* homolog was not present in the zebrafish genome assembly (Zv9) or annotated in the recently published genomic sequence (24).

Using human ChAT as a reference, we searched for conserved amino acid sequences in the zebrafish protein database and identified a region of moderate homology (61% over 103 amino acids) located on contig CABZ01100254.1 adjacent to *vachtb*. Further analyses of contigs in close proximity revealed a second contig, CABZ01100253.1, with homology to the human ChAT sequence (57% over 44 amino acids). Primers were designed against the two regions to amplify the intervening cDNA sequence, resulting in a 1.5-kb fragment. To enrich for *chatb* transcripts, we extracted RNA from Hb microdissected from adults for RNA sequencing (RNA-Seq). The 1.5-kb fragment served as a template for de novo assembly of RNA-Seq reads corresponding to the second *chat* gene. Additional DNA sequencing confirmed the full-length coding sequence. The predicted protein contains a putative catalytical domain (RRLRWK) for ACh synthesis (25), the acyltransferase site (XPXLPXPXL) (26), and a conserved histidine residue that plays a vital role in enzymatic activity (27) (Fig. 1*C* and Fig. S1*B*). The second locus that maps to chromosome 12 is referred to as CGLb (containing *vachtb* and *chatb*).

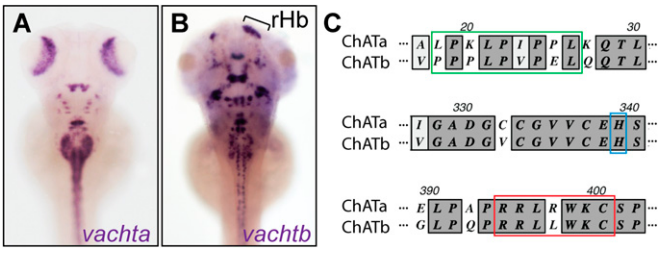

Fig. 1. Duplicated zebrafish ChATb. Distribution of *vachta* (*A*) and *vachtb* (*B*) transcripts in 5-dpf larvae with asymmetrical habenular expression indicated. rHb, right habenula indicated by bracket. (*C*) Alignment of ChATa and ChATb sequences at the acyltransferase site (green), conserved histidine domain (blue), and putative enzyme catalytical domain (red).

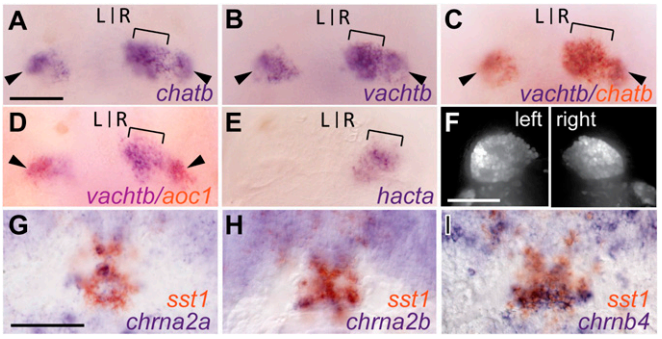

Fig. 2. Cholinergic gene expression in zebrafish Hb-IPN; *chatb* (*A*) and *vachtb* (*B*) transcripts in the right dHb (brackets) and bilaterally in the vHb (arrowheads) of 4-dpf larvae (dorsal views). Double ISH for *vachtb* with *chatb* (*C*) and *aoc1* (*D*). (*E*) *hacta* expression only in right dHb. (*F*) Confocal z-stack images of left and right dHb in *Tg(slc17a6b:DsRed)* larvae. Transverse sections through sst1-expressing IPN of 4-dpf larvae double-labeled for *chrna2a* (*G*), *chrna2b* (*H*), and *chrnb4* (*I*). L, left; R, right. (Scale bars: 50 μm.)

Asymmetrical Expression of CGLb in Larval dHb. The *chatb* gene is expressed throughout the brain in an overlapping pattern with *vachtb* (Fig. 2 *A–C* and Fig. S2 *C–E″*). Double in situ hybridization (ISH) shows that *chata* and *chatb* only colocalize in a cluster of bilaterally paired hindbrain neurons (Fig. S2 *A–C″*), suggesting that most cholinergic neurons express only one *chat* gene. The CGLb genes are also expressed bilaterally in the ventral habenular nuclei (vHb), as demonstrated by coexpression with *amine oxidase, copper containing 1* (*aoc1*) (28) (Fig. 2*D*). However, in the dHb, both *chatb* and *vachtb* are predominantly transcribed on the right side (Fig. 2 *A–C*), indicating that cholinergic neurons are asymmetrically distributed in the larval forebrain.

Cholinergic neurons also synthesize the high-affinity choline transporter (HACT) (29), also known as solute carrier family 5 (choline transporter) member 7, which transports extracellular choline into presynaptic terminals. Zebrafish have two closed related *hact* genes, *hacta* and *hactb*. The *hacta* gene on chromosome 9 is exclusively expressed in the right dHb of larval zebrafish (Fig. 2*E*). However, in contrast to the CGLb genes, *hacta* is not expressed in the vHb.

In rodents, medial habenular neurons express the *vesicular glutamate transporter* (*vglut; slc17a6*) gene (30) and corelease glutamate and ACh (31). Both the left and right dHb are also glutamatergic in zebrafish, as evidenced by labeling of a Vglut2 reporter [*Tg*(*slc17a6b:DsRed*)^{nns9} (32)] (Fig. 2*F*). Thus, only the cholinergic neurotransmitter phenotype appears to be lateralized in the developing dHb.

Select nAChR Subunits in the Larval IPN. The IPN is the major target of dHb neurons and, in mammals, a region where nAChRs are highly enriched (33). To determine whether nAChRs are produced in the zebrafish larval IPN, we examined colocalization of their expression with *somatostatin1* (*sst1*), which is transcribed in neurons throughout the IPN (34, 35). Genes encoding the α2a, α2b, and β4 nAChR subunits were highly expressed in the larval IPN (Fig. 2 *G–I*) at 4 d postfertilization (dpf), the same stage when the CGLb locus is transcriptionally active in the right Hb. This suggests that the asymmetrical Hb-IPN projection is a functional cholinergic pathway.

Sustained Hb Stimulation Induces Slow Cholinergic Currents in the Ventral IPN. To confirm that the larval Hb-IPN tract is functional, we optogenetically activated dHb neurons and measured the electrophysiological response from IPN neurons. The *TgBAC* (*gng8:nfsB-CAAX-GFP*)^{c375} line specifically labels Hb neurons and their axons with membrane-tagged GFP, allowing the IPN to

be identified by its labeled afferents (36). Using the same *gng8* integration site, we generated *TgBAC(gng8:GAL4)*^{c426} to produce Gal4 specifically in Hb neurons at 5-dpf. Upon mating with *Tg(UAS:ChR2(H134R)-mCherry)*$^{s1985t/+}$ carriers, Gal4 drives expression of ChR2 exclusively in Hb neurons. We confirmed ChR2-mCherry labeling of dHb neurons by mating *TgBAC(gng8:GAL4)*^{c426} and *Tg(UAS:ChR2(H134R)-mCherry)*$^{s1985t/+}$ doubly heterozygous fish with *TgBAC(gng8:nfsB-CAAX-GFP)*^{c375} (Fig. 3 *A* and *B*). Because expression from the UAS-regulated transgene was highly variable (33.6 ± 23.4 and 18.9 ± 16.3 labeled cells in the left and right dHb, respectively; $n = 10$), larval brains with the highest number of mCherry-positive neurons were used for electrophysiological recordings.

The right dHb preferentially innervates the ventral IPN (vIPN) (2, 37). We therefore performed whole-cell patch-clamp recordings on neurons in the vIPN following exposure of dissected larval brains to blue-light pulses. As a control, *TgBAC(gng8:nfsB-CAAX-GFP)*^{c375} larvae lacking ChR2 were used to identify and record responses at the vIPN. Currents were not detected following blue-light illumination of control brains ($n = 7$; Fig. 3*C*). In contrast, depolarization of ChR2-mCherry–expressing Hb neurons evoked a bimodal excitatory postsynaptic response in vIPN neurons. Averaged responses exhibited short-lived, fast excitatory postsynaptic currents (EPSCs) and a slow rising and sustained inward current (Fig. 3*D*). The length of illumination (400 ms) was determined as the stimulation duration sufficient for the slow rising inward current to reach maximum amplitude. Blue light-evoked fast EPSCs mostly occurred in a synchronous manner after a fixed delay (average delay of 8.0 ± 1.0 ms) following optical stimulation, with an average amplitude of −11.5 ± 8.7 pA ($n = 7$). The fast EPSCs exhibited an average 10–90% rise time of 0.49 ± 0.07 ms and an average monoexponential decay time constant of 1.45 ± 0.22 ms, suggesting that they were mediated by AMPA-type postsynaptic glutamatergic receptors (38). The slow inward current had an average amplitude of 2.1 ± 1.1 pA and exhibited a monoexponential rise time of 187 ± 38 ms and a decay time constant of 80 ± 18 ms after blue light termination ($n = 5$). Recording at 0 mV upon blue light stimulation revealed outward currents, indicative of $GABA_A$ receptor (GABAR) activation in the vIPN neurons (Fig. S3).

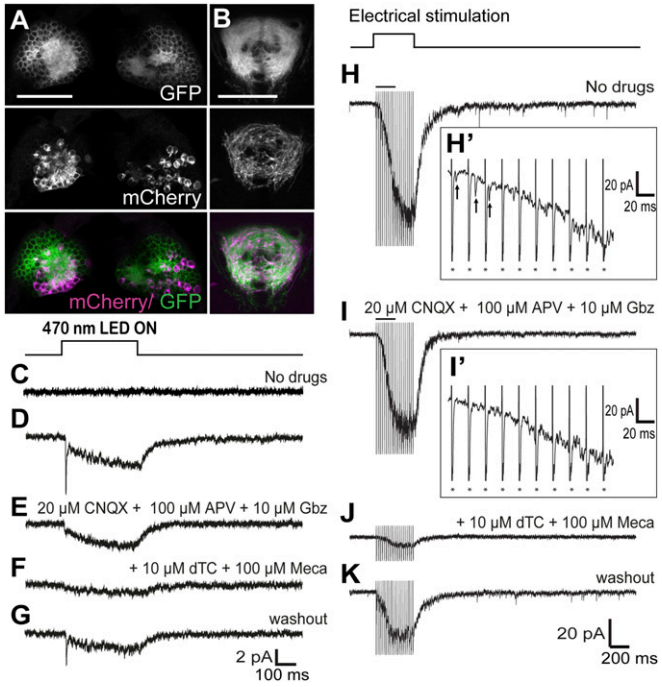

Fig. 3. Sustained Hb stimulation induces slow cholinergic current in the vIPN. Confocal images of the dHb (*A*) and IPN (*B*) of 5-dpf larvae carrying the *TgBAC(gng8:nfsB-CAAX-GFP)*^{c375}, *TgBAC(gng8:GAL4)*^{c426}, and *Tg(UAS:ChR2-mCherry)*$^{s1985t/+}$ transgenes. (Scale bars: 50 μm.) Averages of 15 responses evoked in a vIPN neuron by optogenetic stimulation (400 ms) of Hb neurons in control (*C*) and ChR2-mCherry brains in the absence of drugs (*D*), presence of 20 μM 6-cyano-7-nitroquinoxaline-2,3-dione (CNQX) + 100 μM amino-5-phosphonopentanoic acid (APV) + 10 μM gabazine (Gbz) (*E*), with addition of 10 μM (+)-D-tubocurarine chloride (dTc) + 100 μM mecamylamine (Meca) (*F*), and after washout (*G*). Examples of responses evoked in a single vIPN neuron by repetitive electrical stimulation of the right Hb (400 ms, 50 Hz) without drugs (*H* and *H′*), with 20 μM CNQX + 100 μM APV + 10 μM Gbz (*I* and *I′*), with addition of 10 μM dTc + 100 μM Meca (*J*), and after washout (*K*). *H′* and *I′* are higher resolution traces from *H* and *I*, respectively, illustrating fast EPSCs (*H′*, arrows). Asterisks in *H′* and *I′* mark artifacts of electrical stimulation.

To assess whether the slow rising inward current is cholinergic, we used a pharmacological approach (Fig. 3 *E–G*). ACh-mediated currents were isolated by blocking activity of all glutamate and kainate receptors (20 μM 6-cyano-7-nitroquinoxaline-2,3-dione and 100 μM amino-5-phosphonopentanoic acid) as well as $GABA_A$ receptors (10 μM Gbz). Fast EPSCs evoked by blue light stimulation were no longer observed, indicative of the glutamate receptor blockade. The slow rising inward current was decreased by 44 ± 33% but was still clearly detectable ($n = 4$). However, upon addition of nAChR antagonists [100 μM mecamylamine and 10 μM (+)-D-tubocurarine chloride], the slow inward current was significantly inhibited by 83 ± 10% ($n = 4$; $P < 0.01$, two-tailed paired *t* test), indicating that it was cholinergic. Washout for 20–30 min allowed a partial recovery of fast EPSCs (27 ± 16% of initial response) and the slow inward current (31 ± 19%, $n = 3$).

Unilateral electrical stimulation provided additional evidence that neurons in the right dHb induce cholinergic currents in vIPN neurons. Direct stimulation of the right Hb (50-Hz pulse for 400 ms; Fig. 3*H*) evoked not only fast EPSCs (Fig. 3*H′*) but slow inward currents that were much larger (61 ± 29 pA, $n = 7$) than those obtained with optogenetic activation. In the presence of glutamatergic and GABAergic antagonists (Fig. 3 *I* and *I′*), fast EPSCs were completely lost and the slow current was partially reduced (25 ± 17%, $n = 5$). The remaining slow inward current was largely blocked by nAChR antagonists (89 ± 3%, $n = 5$; Fig. 3*J*). The slow current (32 ± 5% of the initial amplitude; Fig. 3*K*) partially recovered following washout for 20–30 min. These results indicate that cholinergic neurons in the right dHb release ACh upon stimulation of the larval brain and that nAChRs in the IPN are functional at this early stage of development. Stimulation of the left dHb elicited similar responses, albeit of much lower magnitude (14 ± 7 pA, $n = 6$), likely owing to current passage through the habenular commissure or direct activation of the small cholinergic population on the left side.

Discrete Cholinergic and Peptidergic Subnuclei in the dHb. To test whether the L-R difference in cholinergic neurons persists, expression of the CGLb and *hacta* genes was examined in adults. As in larvae, both vHb express *vachtb* and *chatb.* However, in contrast to the asymmetrical expression observed in the larval dHb, *vachtb*, *chatb*, and *hacta* transcripts are found in subregions of the left dHb as well as the right dHb (Fig. 4 *A–C*).

The mHb of rodents can be subdivided into distinct cholinergic and substance P (SP) domains (11). To determine whether the noncholinergic neurons of the left dHb are peptidergic, we examined expression of *tachykinin1* (*tac1*), which generates a precursor mRNA encoding for both the SP and neurokinin A peptides. Transcripts for *tac1* localized to a large domain in the left dHb and to a smaller one in the right dHb, in regions devoid of *vachtb* expression (Fig. 4*D*).

To examine whether neurons within the cholinergic region of the dHb show distinct patterns of connectivity, we used *Tg* (*brn3a-hsp70:GFP*), which labels neurons in the medial dHb (dHbM) and their projections to the iIPN and vIPN (37). We find that the vast majority of *vachtb*-expressing neurons are GFP-positive in the left and right dHb of *Tg*(*brn3a-hsp70:GFP*) adults (Fig. 4 *E* and *F*). The cholinergic neurons are therefore located in the dHbM and mainly innervate the iIPN and vIPN.

Preferential Nicotine-Induced Neuronal Activity in the iIPN. The Hb-IPN pathway is involved in nicotine addiction (5), and activation of IPN neurons limits nicotine intake in mice (39). To assess the responsiveness of IPN neurons to nicotine, we exposed adults to the drug and assayed expression of *fos*, an immediate early gene up-regulated upon neuronal activation. In contrast to controls, we observed a striking number of *fos*-expressing cells in the IPN of nicotine-treated animals (control = 1.2 ± 1, $n = 6$; nicotine-treated = 56.2 ± 8.4, $n = 6$; Fig. 5 *G* and *H*), which were concentrated in the iIPN subregion [iIPN = 36.6 ± 5.6; dorsal IPN (dIPN) = 7.7 ± 2; vIPN = 11.9 ± 2.5, $n = 6$].

We determined whether nicotine-induced activation of *fos* in the iIPN corresponded with expression of nAChR subunits. The *chrna2a*, *chrna2b*, *chrnb4*, *chrna5*, and *chrna7* genes, as well as *acetylcholine esterase* (*ache*), are mainly expressed in the vIPN and ventral half of the iIPN, whereas *chrnb2b* is expressed in the dIPN and dorsal half of the iIPN (Fig. 5 *A*–*F*′). As in rodents, *chrna3* is not expressed in the IPN. Double labeling confirmed that *chrna2b* and *fos* transcripts colocalize. Of the *fos*-positive iIPN neurons, 78.6 ± 0.1% also expressed *chrna2b* ($n = 7$; 321 cells; Fig. 5*I*), indicating that nicotine induces preferential activation of *chrna2b*-expressing iIPN neurons. These findings indicate that different subregions of the adult IPN express specific nAChR subunits, which differ in their sensitivity to nicotinic activation.

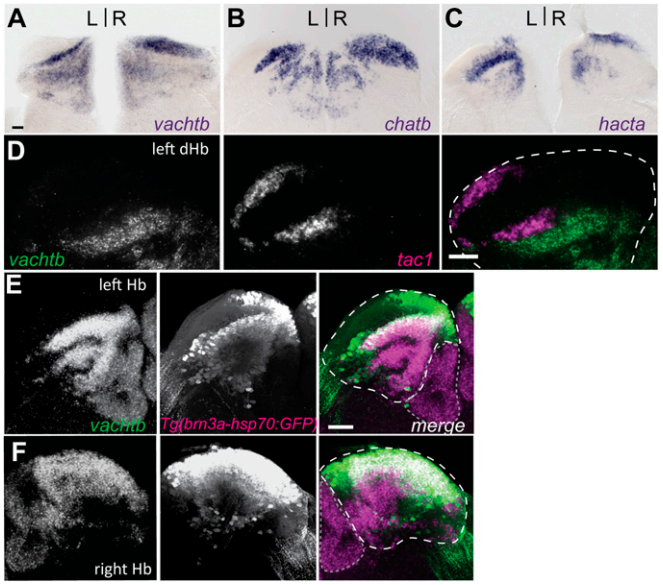

Fig. 4. Discrete cholinergic and peptidergic subnuclei of adult dHb. Transverse sections through the Hb of adult brains processed for *vactb* (*A*), *chatb* (*B*), and *hacta* (*C*) expression. (*D*) Double fluorescent ISH for *vachtb* and *tac1* confirm nonoverlapping cholinergic (green) and *tac1*-positive (magenta) neuronal populations in the left dHb. Composite z-stack images taken from coronal sections of left (*E*) and right (*F*) Hb. Coexpression of *vachtb* (magenta) and Tg(*brn3a-hsp70:GFP*) (green). (*D*–*F*) White dashed lines delineate dHb, and gray dotted lines delineate vHb. (Scale bars: 50 μm.)

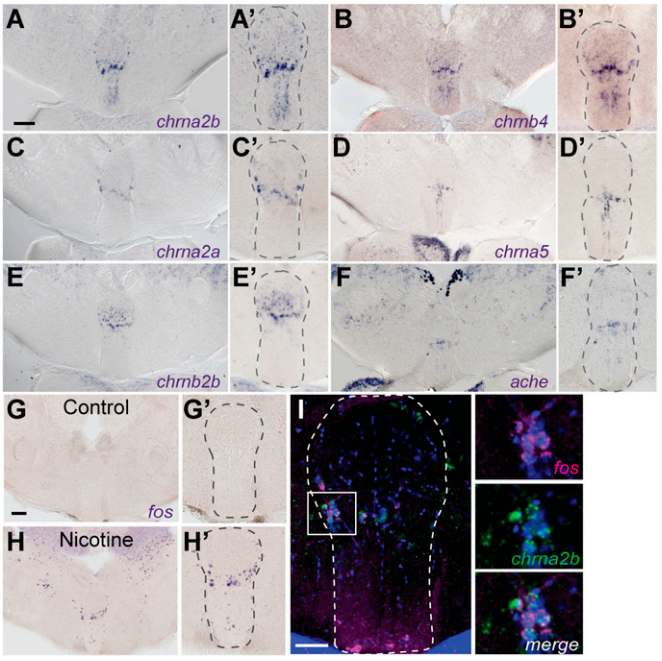

Fig. 5. Nicotine-responsive neurons localize to iIPN. Transverse sections of adult brain show *chrna2b* (*A* and *A*′), *chrnb4* (*B* and *B*′), *chrna2a* (*C* and *C*′), *chrna5* (*D* and *D*′), *chrnb2b* (*E* and *E*′), and *ache* (*F* and *F*′) transcripts. Control (*G* and *G*′) and nicotine-treated (*H* and *H*′) fish were processed for *fos* expression. (Scale bars: *A* and *G*, 100 μm.) (*A*′–*H*′) Enlarged images of the IPN. (*I*) Double fluorescent ISH shows *fos* (magenta) and *chrna2b* (green) colocalization. DAPI labeling is in blue. The white box in *I* corresponds to enlarged panels on the right. (Scale bar: 50 μm.) Dotted lines delineate the IPN.

Discussion

This study resolves a long-standing question concerning the cholinergic identity of the dHb of zebrafish, through the characterization of a duplicated CGL. Our findings not only support a conserved role for ACh in the dHb-IPN tract of vertebrates but reveal L-R differences in the distribution of cholinergic neurons in the developing and adult brain.

Although sequencing of the zebrafish genome had not demonstrated a second CGL (24), several lines of evidence support its presence. The *vachtb* and *chatb* genes are in close proximity and bounded by genes that are syntenic with those that flank CGLa. Similarity among predicted amino acid sequences is ∼75% for *vachta* and *vachtb* coding regions and 50% for *chata* and *chatb* coding regions. Further, *chatb* encodes a protein that contains structural and enzymatic motifs essential for activity (25–27).

ChAT and VAChT are coexpressed in a wide array of neuronal populations (40). In many species, *vacht* is located in the first intronic region of *chat* (41–44), suggesting transcriptional coregulation. However, temporal and spatial discrepancies in expression of the two genes suggest more complicated regulation (45–47). In zebrafish larvae, all *chatb*-expressing neurons coexpress *vachtb*, but *vachtb* transcripts are also found in *chata*-expressing regions, such as the retina and nucleus of the medial longitudinal fascicle. Thus, in most but not all cholinergic neuronal populations, the *chat* and *vacht* genes of a given CGL appear to be coexpressed.

The two zebrafish *chat* homologs are largely transcribed in distinct neuronal populations in the larval nervous system, suggesting that only one ChAT is synthesized by individual cholinergic neurons. In humans, seven different transcripts have been identified from the single *chat* gene, which encode at least three different proteins (48–50). ChAT isoforms have also been identified in other species (51, 52), such as the pChAT splice

variant of rats specific to the peripheral nervous system (53). The catalytical activity rate of ChAT is ~3,000-fold greater than that of pChAT (54, 55). Conceivably, zebrafish ChATa and ChATb could differ in their rate or efficiency of ACh synthesis.

Divergence of the two CGLs and their expression in largely distinct cholinergic populations may be an additional mechanism to refine modulation of cholinergic neurotransmission. Two major parallel tracts connect the mHb and IPN in mammals (56). Projections from the triangular septum to a cholinergic Hb subdomain innervate the medial IPN, whereas the bed nucleus of the anterior commissure targets an SP-expressing Hb subdomain that innervates the lateral IPN. The two pathways play distinct roles, with the former regulating anxiety and the latter modulating fear responses and learning (56).

In zebrafish, habenular subdomains have been defined using transgenic lines and gene expression patterns. In *Tg*(*brn3a-hsp70:GFP*) individuals, GFP is expressed in a subset of dHb neurons that mainly project to the iIPN/vIPN (37). Conversely, dHb neurons expressing the *neural activity-related petaxin* (*narp*) gene are devoid of GFP labeling and mainly project to the iIPN/dIPN (57). On this basis, the *brn3a:GFP* and *narp* domains were designated as dHbM and lateral dHb (dHbL). The dHbL was implicated in mediating fear responses of zebrafish (57) comparable to the role of the rodent medial dorsal (SP) subnucleus, suggesting functional homology between these brain regions. However, because *tac1* transcripts were not detected in the zebrafish Hb (58) and their cholinergic nature was also unresolved (13–15), functional comparisons with the mammalian Hb were incomplete.

We now show that CGLb and *tac1*-expressing populations are segregated in the dHb of adult zebrafish as in the mammalian brain (11). Analyses in the *Tg*(*brn3a-hsp70:GFP*) line indicate that cholinergic subnuclei project to the iIPN/vIPN (37). The *tac1*-expressing region overlaps with the *narp*-expressing dHbL subdomain, suggesting that peptidergic neurons project to the iIPN/dIPN. From their neurochemical properties and patterns of connectivity, the zebrafish dHbM and dHbL are therefore homologous to the cholinergic ventral mHb and SP-producing dorsal mHb of the mammalian brain, respectively. However, in contrast to the seemingly bilaterally symmetrical Hb of rodents, the peptidergic and cholinergic subnuclei of the zebrafish brain differ in size on the left and right sides. The ability to alter the directionality or degree of asymmetry in the zebrafish epithalamus will facilitate functional studies on the behavioral significance of L-R differences in these distinct neuronal populations.

Subtle L-R differences in levels of neurotransmitters or their receptors have been observed in the mammalian brain. In rodents, dopamine levels in the nucleus accumbens (59) and muscarinic binding affinity in the hippocampus (60) differ on the left and right. Levels of ChAT, glutamic acid decarboxylase, GABA, and dopamine also vary between the human brain hemispheres (61). Remarkably, mice exhibit learning and memory deficits when L-R differences in the distribution of *N*-methyl-D-aspartate receptor ε2 subunit are altered in hippocampal neurons (62, 63). Thus, differences in neurotransmitter synthesis, distribution, and release between hemispheres may be a more general mechanism for regulating neuronal activity and behavior.

Optogenetic or electrical stimulation of the dHb of zebrafish larvae generated glutamatergic and cholinergic currents in the vIPN. Individual neurons in the mHb of the adult mouse brain also elicit fast glutamatergic currents, together with a slow cholinergic current at the IPN (31). Specific nAChR subtypes account for this cholinergic response. Only *chrna2a*, *chrna2b*, and *chrnb4* transcripts were detected in the IPN of larval zebrafish. In addition to expressing more subunit types, varying combinations of transcripts were found in subregions of the adult brain. Expression and pharmacological studies in the mouse have also suggested that the IPN consists of discrete domains differing in nAChR subunit composition (20, 64, 65).

Following exposure to nicotine, adult zebrafish preferentially up-regulate *fos* expression in the iIPN, supporting that the IPN consists of heterogeneous neuronal populations. Coexpression of *chrna2b* and *fos* suggests that nicotine either directly causes postsynaptic activation of IPN neurons or indirectly induces *fos* expression through presynaptic activation of habenular neurons that innervate *chrna2b*-expressing iIPN neurons. We favor the latter hypothesis, because glutamate release in the mouse IPN is regulated by binding of nicotine to nAChRs containing the a5 subunit, located at habenular axon terminals (66).

Specific nAChRs subunits have been implicated in facilitating nicotine withdrawal symptoms. Mice that lack the *chrna2*, *chrna5*, or *chrnb4* subunit show attenuated symptoms, whereas *chrnb2* and *chrna7* mutants show no difference (67–69). Although these subunits are expressed in other areas of the brain, only in the Hb-IPN pathway are they coexpressed (20, 70, 71). Reintroduction of the α5 subunit in the Hb of the *chrna5* mutant mouse is sufficient to rescue the altered response to nicotine. Notably, the two subunits responsible for differences in nicotine-mediated behavior in rodents, *chrna2* and *chrnb4*, also have the highest transcript levels in the zebrafish iIPN. It was previously proposed that zebrafish provide a useful system to study nicotine addiction (72, 73). This claim is greatly strengthened by our demonstration of the Hb-IPN pathway as cholinergic, firmly establishing the zebrafish as a valid model for dissecting the molecular and neuronal bases of nicotine addiction.

Materials and Methods

Fish strains used in this study and the generation of the transgenic line *TgBAC (gng8:GAL4)c426* are described in *SI Materials and Methods*. RNA-Seq and data analyses for identification of *chatb* are also provided. Protocols are also outlined in *SI Materials and Methods* for RNA ISH, brain sectioning, microscopy, nicotine treatment, optogenetic activation of the Hb and electrophysiology of IPN neurons.

ACKNOWLEDGMENTS. We thank Frederick Tan, Nicolas Ingolia, and Allison Pinder for assistance with RNA-Seq and data analysis; Pascal Legendre for advice on electrophysiology experiments; Estela Monge and Michelle Macurak for technical support; and Harold Burgess, Tagide deCarvalho, Erik Duboué, and Rejji Kuruvilla for helpful comments on the manuscript. Hitoshi Okamoto and Yoshihiro Yoshihara provided *Tg*(*brn3a-hsp70:GFP*)^{rw0110b} and *Tg*(*slc17a6b:DsRed*)^{nns9}, and Tom Boyd provided the *chrna2a* and *chrna7* plasmids. This study was supported by European Molecular Biology Organization Short-Term Fellowship 517-2012 (to E.H.), University of Virginia funds (to C.T. and B.T.), and National Institutes of Health Grants 5R01HD042215 and 5R01HD058530 (to M.E.H.).

1. Signore IA, et al. (2009) Zebrafish and medaka: Model organisms for a comparative developmental approach of brain asymmetry. *Philos Trans R Soc Lond B Biol Sci* 364(1519):991–1003.
2. Gamse JT, et al. (2005) Directional asymmetry of the zebrafish epithalamus guides dorsoventral innervation of the midbrain target. *Development* 132(21):4869–4881.
3. Concha ML, Wilson SW (2001) Asymmetry in the epithalamus of vertebrates. *J Anat* 199(Pt 1-2):63–84.
4. Sutherland RJ (1982) The dorsal diencephalic conduction system: A review of the anatomy and functions of the habenular complex. *Neurosci Biobehav Rev* 6(1):1–13.
5. Baldwin PR, Alanis R, Salas R (2011) The Role of the Habenula in Nicotine Addiction. *J Addict Res Ther* S1(2).
6. Heckers S, Geula C, Mesulam MM (1992) Cholinergic innervation of the human thalamus: Dual origin and differential nuclear distribution. *J Comp Neurol* 325(1):68–82.
7. Sorenson EM, Parkinson D, Dahl JL, Chiappinelli VA (1989) Immunohistochemical localization of choline acetyltransferase in the chicken mesencephalon. *J Comp Neurol* 281(4):641–657.
8. Marín O, Smeets WJ, González A (1997) Distribution of choline acetyltransferase immunoreactivity in the brain of anuran (Rana perezi, Xenopus laevis) and urodele (Pleurodeles waltl) amphibians. *J Comp Neurol* 382(4):499–534.
9. López JM, Domínguez L, Morona R, Northcutt RG, González A (2012) Organization of the cholinergic systems in the brain of two lungfishes, Protopterus dolloi and Neoceratodus forsteri. *Brain Struct Funct* 217(2):549–576.
10. Villani L, Battistini S, Bissoli R, Contestabile A (1987) Cholinergic projections in the telencephalo-habenulo-interpeduncular system of the goldfish. *Neurosci Lett* 76(3): 263–268.

11. Cuello AC, Emson PC, Paxinos G, Jessell T (1978) Substance P containing and cholinergic projections from the habenula. *Brain Res* 149(2):413–429.
12. Yokogawa T, et al. (2007) Characterization of sleep in zebrafish and insomnia in hypocretin receptor mutants. *PLoS Biol* 5(10):e277.
13. Arenzana FJ, et al. (2005) Development of the cholinergic system in the brain and retina of the zebrafish. *Brain Res Bull* 66(4-6):421–425.
14. Mueller T, Vernier P, Wullimann MF (2004) The adult central nervous cholinergic system of a neurogenetic model animal, the zebrafish Danio rerio. *Brain Res* 1011(2): 156–169.
15. Clemente D, et al. (2004) Cholinergic elements in the zebrafish central nervous system: Histochemical and immunohistochemical analysis. *J Comp Neurol* 474(1):75–107.
16. Zirger JM, Beattie CE, McKay DB, Boyd RT (2003) Cloning and expression of zebrafish neuronal nicotinic acetylcholine receptors. *Gene Expr Patterns* 3(6):747–754.
17. Papke RL, Ono F, Stokes C, Urban JM, Boyd RT (2012) The nicotinic acetylcholine receptors of zebrafish and an evaluation of pharmacological tools used for their study. *Biochem Pharmacol* 84(3):352–365.
18. Yeh JJ, et al. (2001) Neuronal nicotinic acetylcholine receptor alpha3 subunit protein in rat brain and sympathetic ganglion measured using a subunit-specific antibody: Regional and ontogenic expression. *J Neurochem* 77(1):336–346.
19. Cui C, et al. (2003) The beta3 nicotinic receptor subunit: A component of alpha-conotoxin MII-binding nicotinic acetylcholine receptors that modulate dopamine release and related behaviors. *J Neurosci* 23(35):11045–11053.
20. Wada E, et al. (1989) Distribution of alpha 2, alpha 3, alpha 4, and beta 2 neuronal nicotinic receptor subunit mRNAs in the central nervous system: A hybridization histochemical study in the rat. *J Comp Neurol* 284(2):314–335.
21. Le Novère N, Zoli M, Changeux JP (1996) Neuronal nicotinic receptor alpha 6 subunit mRNA is selectively concentrated in catecholaminergic nuclei of the rat brain. *Eur J Neurosci* 8(11):2428–2439.
22. Whiteaker P, et al. (2002) Involvement of the alpha3 subunit in central nicotinic binding populations. *J Neurosci* 22(7):2522–2529.
23. Thisse B, et al. (2004) Spatial and temporal expression of the zebrafish genome by large-scale in situ hybridization screening. *Methods Cell Biol* 77:505–519.
24. Howe K, et al. (2013) The zebrafish reference genome sequence and its relationship to the human genome. *Nature* 496(7446):498–503.
25. Ishii K, Oda Y, Ichikawa T, Deguchi T (1990) Complementary DNAs for choline acetyltransferase from spinal cords of rat and mouse: Nucleotide sequences, expression in mammalian cells, and in situ hybridization. *Brain Res Mol Brain Res* 7(2):151–159.
26. Finocchiaro G, et al. (1991) cDNA cloning, sequence analysis, and chromosomal localization of human carnitine palmitoyltransferase. *Proc Natl Acad Sci USA* 88(23): 10981.
27. Malthe-Sorenssen D (1976) Choline acetyltransferase—Evidence for acetyl transfer by a histidine residue. *J Neurochem* 27(4):873–881.
28. Amo R, et al. (2010) Identification of the zebrafish ventral habenula as a homolog of the mammalian lateral habenula. *J Neurosci* 30(4):1566–1574.
29. Atweh S, Simon JR, Kuhar MJ (1975) Utilization of sodium-dependent high affinity choline uptake in vitro as a measure of the activity of cholinergic neurons in vivo. *Life Sci* 17(10):1535–1544.
30. Qin C, Luo M (2009) Neurochemical phenotypes of the afferent and efferent projections of the mouse medial habenula. *Neuroscience* 161(3):827–837.
31. Ren J, et al. (2011) Habenula "cholinergic" neurons co-release glutamate and acetylcholine and activate postsynaptic neurons via distinct transmission modes. *Neuron* 69(3):445–452.
32. Miyasaka N, et al. (2009) From the olfactory bulb to higher brain centers: Genetic visualization of secondary olfactory pathways in zebrafish. *J Neurosci* 29(15):4756–4767.
33. Pauly JR, Stitzel JA, Marks MJ, Collins AC (1989) An autoradiographic analysis of cholinergic receptors in mouse brain. *Brain Res Bull* 22(2):453–459.
34. Hemmendinger LM, Moore RY (1984) Interpeduncular nucleus organization in the rat: Cytoarchitecture and histochemical analysis. *Brain Res Bull* 13(1):163–179.
35. Doll CA, Burkart JT, Hope KD, Halpern ME, Gamse JT (2011) Subnuclear development of the zebrafish habenular nuclei requires ER translocon function. *Dev Biol* 360(1): 44–57.
36. Decarvalho TN, Akitake CM, Thisse C, Thisse B, Halpern ME (2013) Aversive cues fail to activate fos expression in the asymmetric olfactory-habenula pathway of zebrafish. *Front Neural Circuits* 7:98.
37. Aizawa H, et al. (2005) Laterotopic representation of left-right information onto the dorso-ventral axis of a zebrafish midbrain target nucleus. *Curr Biol* 15(3):238–243.
38. Traynelis SF, et al. (2010) Glutamate receptor ion channels: Structure, regulation, and function. *Pharmacol Rev* 62(3):405–496.
39. Fowler CD, Lu Q, Johnson PM, Marks MJ, Kenny PJ (2011) Habenular α5 nicotinic receptor subunit signalling controls nicotine intake. *Nature* 471(7340):597–601.
40. Ichikawa T, Ajiki K, Matsuura J, Misawa H (1997) Localization of two cholinergic markers, choline acetyltransferase and vesicular acetylcholine transporter in the central nervous system of the rat: In situ hybridization histochemistry and immunohistochemistry. *J Chem Neuroanat* 13(1):23–39.
41. Erickson JD, et al. (1994) Functional identification of a vesicular acetylcholine transporter and its expression from a "cholinergic" gene locus. *J Biol Chem* 269(35): 21929–21932.
42. Bejanin S, Cervini R, Mallet J, Berrard S (1994) A unique gene organization for two cholinergic markers, choline acetyltransferase and a putative vesicular transporter of acetylcholine. *J Biol Chem* 269(35):21944–21947.
43. Naciff JM, Misawa H, Dedman JR (1997) Molecular characterization of the mouse vesicular acetylcholine transporter gene. *Neuroreport* 8(16):3467–3473.
44. Kitamoto T, Wang W, Salvaterra PM (1998) Structure and organization of the Drosophila cholinergic locus. *J Biol Chem* 273(5):2706–2713.
45. Holler T, Berse B, Cermak JM, Diebler MF, Blusztajn JK (1996) Differences in the developmental expression of the vesicular acetylcholine transporter and choline acetyltransferase in the rat brain. *Neurosci Lett* 212(2):107–110.
46. Erickson JD, et al. (1996) The VAChT/ChAT "cholinergic gene locus": New aspects of genetic and vesicular regulation of cholinergic function. *Prog Brain Res* 109:69–82.
47. Schütz B, Weihe E, Eiden LE (2001) Independent patterns of transcription for the products of the rat cholinergic gene locus. *Neuroscience* 104(3):633–642.
48. Misawa H, Matsuura J, Oda Y, Takahashi R, Deguchi T (1997) Human choline acetyltransferase mRNAs with different 5′-region produce a 69-kDa major translation product. *Brain Res Mol Brain Res* 44(2):323–333.
49. Oda Y, Muroishi Y, Misawa H, Suzuki S (2004) Comparative study of gene expression of cholinergic system-related molecules in the human spinal cord and term placenta. *Neuroscience* 128(1):39–49.
50. Gill SK, et al. (2007) 82-kDa choline acetyltransferase is in nuclei of cholinergic neurons in human CNS and altered in aging and Alzheimer disease. *Neurobiol Aging* 28(7):1028–1040.
51. Misawa H, Ishii K, Deguchi T (1992) Gene expression of mouse choline acetyltransferase. Alternative splicing and identification of a highly active promoter region. *J Biol Chem* 267(28):20392–20399.
52. Kengaku M, Misawa H, Deguchi T (1993) Multiple mRNA species of choline acetyltransferase from rat spinal cord. *Brain Res Mol Brain Res* 18(1-2):71–76.
53. Tooyama I, Kimura H (2000) A protein encoded by an alternative splice variant of choline acetyltransferase mRNA is localized preferentially in peripheral nerve cells and fibers. *J Chem Neuroanat* 17(4):217–226.
54. Bellier JP, Kimura H (2011) Peripheral type of choline acetyltransferase: Biological and evolutionary implications for novel mechanisms in cholinergic system. *J Chem Neuroanat* 42(4):225–235.
55. Eckenstein F, Thoenen H (1982) Production of specific antisera and monoclonal antibodies to choline acetyltransferase: Characterization and use for identification of cholinergic neurons. *EMBO J* 1(3):363–368.
56. Yamaguchi T, Danjo T, Pastan I, Hikida T, Nakanishi S (2013) Distinct roles of segregated transmission of the septo-habenular pathway in anxiety and fear. *Neuron* 78(3):537–544.
57. Agetsuma M, et al. (2010) The habenula is crucial for experience-dependent modification of fear responses in zebrafish. *Nat Neurosci* 13(11):1354–1356.
58. Ogawa S, et al. (2012) Cloning and expression of tachykinins and their association with kisspeptins in the brains of zebrafish. *J Comp Neurol* 520(13):2991–3012.
59. Budilin SY, Midzyanovskaya IS, Shchegolevskii NV, Ioffe ME, Bazyan AS (2008) Asymmetry in dopamine levels in the nucleus accumbens and motor preference in rats. *Neurosci Behav Physiol* 38(9):991–994.
60. Wolff SC, Hruska Z, Nguyen L, Dohanich GP (2008) Asymmetrical distributions of muscarinic receptor binding in the hippocampus of female rats. *Eur J Pharmacol* 588(2-3):248–250.
61. Glick SD, Ross DA, Hough LB (1982) Lateral asymmetry of neurotransmitters in human brain. *Brain Res* 234(1):53–63.
62. Kawakami R, et al. (2003) Asymmetrical allocation of NMDA receptor epsilon2 subunits in hippocampal circuitry. *Science* 300(5621):990–994.
63. Goto K, et al. (2010) Left-right asymmetry defect in the hippocampal circuitry impairs spatial learning and working memory in iv mice. *PLoS ONE* 5(11):e15468.
64. Salminen O, Seppä T, Gäddnäs H, Ahtee L (2000) Effect of acute nicotine on Fos protein expression in rat brain during chronic nicotine and its withdrawal. *Pharmacol Biochem Behav* 66(1):87–93.
65. Rotter A, Jacobowitz DM (1984) Localization of substance P, acetylcholinesterase, muscarinic receptors and alpha-bungarotoxin binding sites in the rat interpeduncular nucleus. *Brain Res Bull* 12(1):83–94.
66. Girod R, Barazangi N, McGehee D, Role LW (2000) Facilitation of glutamatergic neurotransmission by presynaptic nicotinic acetylcholine receptors. *Neuropharmacology* 39(13):2715–2725.
67. Salas R, Pieri F, De Biasi M (2004) Decreased signs of nicotine withdrawal in mice null for the beta4 nicotinic acetylcholine receptor subunit. *J Neurosci* 24(45):10035–10039.
68. Salas R, Main A, Gangitano D, De Biasi M (2007) Decreased withdrawal symptoms but normal tolerance to nicotine in mice null for the alpha7 nicotinic acetylcholine receptor subunit. *Neuropharmacology* 53(7):863–869.
69. Salas R, Sturm R, Boulter J, De Biasi M (2009) Nicotinic receptors in the habenulo-interpeduncular system are necessary for nicotine withdrawal in mice. *J Neurosci* 29(10):3014–3018.
70. Wada E, McKinnon D, Heinemann S, Patrick J, Swanson LW (1990) The distribution of mRNA encoded by a new member of the neuronal nicotinic acetylcholine receptor gene family (alpha 5) in the rat central nervous system. *Brain Res* 526(1):45–53.
71. Winzer-Serhan UH, Leslie FM (1997) Codistribution of nicotinic acetylcholine receptor subunit alpha3 and beta4 mRNAs during rat brain development. *J Comp Neurol* 386(4):540–554.
72. Klee EW, Ebbert JO, Schneider H, Hurt RD, Ekker SC (2011) Zebrafish for the study of the biological effects of nicotine. *Nicotine Tob Res* 13(5):301–312.
73. Ninkovic J, Bally-Cuif L (2006) The zebrafish as a model system for assessing the reinforcing properties of drugs of abuse. *Methods* 39(3):262–274.